THE JOURNAL OF BIOLOGICAL CHEMISTRY
Vol. 279, No. 23, Issue of June 4, pp. 24313–24322, 2004
Printed in U.S.A.
© 2004 by The American Society for Biochemistry and Molecular Biology, Inc.

Identification of an Interleukin-15α Receptor-binding Site on Human Interleukin-15*

Received for publication, November 13, 2003, and in revised form, March 2, 2004
Published, JBC Papers in Press, March 23, 2004, DOI 10.1074/jbc.M312458200

Jérôme Bernard‡§, Catherine Harb‡, Erwan Mortier‡¶, Agnès Quéméner‡, Rob H. Meloen‖, Claudine Vermot-Desroches, John Wijdeness**, Peter van Dijken‖, Joachim Grötzinger‡‡, Jerry W. Slootstra‖, Ariane Plet‡, and Yannick Jacques‡§§**

*From the ‡Groupe de Recherche Cytokines et Récepteurs, Unité INSERM 601, Institut de Biologie, 9 Quai Moncousu, 44093 Nantes Cedex 01, France, ‖Pepscan Systems, Edelhertweg 15, 8219 PH Lelystad, The Netherlands, **Diaclone, 1 Bld A. Fleming, BP 1985, 25020 Besançon Cedex, France, and the ‡‡Department of Biochemistry, Christian-Albrechts-Universität zu Kiel, Olshausenstrasse 40, D-24098, Kiel, Germany*

To identify the epitopes in human interleukin-15 (IL-15) that are responsible for binding to the interleukin-15 receptor α chain, antibody and receptor mapping by peptide scanning and site-directed mutagenesis was used. By using peptide scanning, we identified four regions in IL-15. The first region (^{85}CKECEELEEKN^{95}) is located in the C-D loop and is recognized by a set of non-inhibitory antibodies. The second region (^{102}SFVHIVQMFIN^{112}) is located in helix D and is recognized by two antibodies that are inhibitory of IL-15 bio-activity but not of IL-15 binding to IL-15Rα. The two remaining regions react with a recombinant soluble form of the IL-15Rα; the first (^{44}LLELQVISL^{52}, peptide 1) corresponds to a sequence located in the B-helix and the second (^{64}ENLII^{68}, peptide 2) to a sequence located in helix C. The latter is also contained in the epitope recognized by an antibody (monoclonal antibody B-E29) that prevents IL-15 binding to IL-15Rα. By site-directed mutagenesis, we confirmed that residues present in peptide 1 (Leu-45, Glu-46, Val-49, Ser-51, and Leu-52) and peptide 2 (Leu-66 and Ile-67) are involved in the binding of IL-15 to IL-15Rα. Furthermore, the results presented indicate that residues in the second peptide (Glu-64, Asn-65, and Ile-68) participate in IL-2Rβ recruitment. This finding could have implications for the dynamics of receptor assembly. These results also indicate that the modes of interaction of IL-15 and IL-2 with their respective α chains are not completely analogous. Finally, some of the IL-15 mutants generated in this study displayed agonist or antagonist properties and may be useful as therapeutic agents.

Interleukin-15 (IL-15)[1] was identified as a new cytokine able to replace IL-2 in supporting the proliferation of a murine T cell line (1, 2). Both cytokines are structurally related and belong to the four α-helix bundle family (3). IL-15 was subsequently found to mimic most of the *in vitro* activities elicited by IL-2 *in vitro*, including induction of proliferation and cytotoxicity by activated T cells (1) and NK cells (2, 4), co-stimulation of B cell proliferation and immunoglobulin synthesis (5), and chemoattraction for T cells (6). This redundancy is explained by the common usage within their functional receptors of the IL-2Rβ/γ signaling complex. This IL-2Rβ/γ complex is a common intermediate affinity receptor for IL-2 and IL-15 (K_d = 1 nM), and both cytokines compete to bind to this receptor (7). Cytokine specificity is conferred by additional private chains, IL-2Rα and IL-15Rα, that are structurally related (8). These two chains contain structural domains (called sushi domains) previously found in some complement and adhesion molecules (9). IL-2Rα contains two such domains, whereas IL-15Rα contains only one. One noticeable difference is that IL-2 binds to its specific IL-2Rα with an affinity (K_d = 10 nM) far lower than IL-15 to IL-15Rα (K_d = 0.05 nM). Each specific chain can associate with the IL-2Rβ/γ complex to form a cytokine-specific, functional high affinity (αβγ) receptor (10–12). Because of the sharing of this IL-2Rβ/γ complex, both cytokines trigger similar downstream signaling pathways including activation of Jak-1/Jak-3 tyrosine kinases and subsequent nuclear translocation of the phosphorylated Stat-3 and Stat-5, activation of lymphocyte-specific tyrosine kinase and spleen tyrosine kinases, activation of the mitogen-activated protein kinase pathway, and induction of B cell leukemia-2 (13, 14). In contrast to IL-2Rβ and IL-2Rγ that are required for signal transduction, the specific receptors IL-2Rα and IL-15Rα have short intracellular tails (13 and 41 amino acids, respectively), and IL-2Rα is considered to play no role in signal transduction. Although initial studies have pointed out the dispensable role of the intracellular tail of IL-15Rα in signaling (8), more recent data suggest that IL-15Rα might mediate certain intracellular functions (15–17).

In contrast to the general functional redundancy observed *in vitro*, several findings point to complementary and even opposing actions of IL-2 and IL-15 *in vivo*. Indeed, whereas IL-2 and IL-2Rα gene expression is mainly restricted to the activated T cell compartment, IL-15 and IL-15Rα transcripts are expressed by various cell types and tissues (monocytes, dendritic and stromal cells, keratinocytes, placenta, skeletal muscle, and heart) suggesting additional roles for the IL-15 system beyond the immune system (7, 8). Cells expressing IL-15Rα in the absence of IL-2Rβ and/or IL-2Rγ have been described, and

* This work was supported in part by Grant P00/3/5692 from the Association pour la Recherche sur le Cancer, INSERM, and CNRS. The costs of publication of this article were defrayed in part by the payment of page charges. This article must therefore be hereby marked "*advertisement*" in accordance with 18 U.S.C. Section 1734 solely to indicate this fact.

§ Recipient of fellowships from the Ligue Nationale Contre le Cancer (Comité de Vendée) and from the ARC.

¶ Recipient of a fellowship from the Ministère de la Recherche et des Nouvelles Technologies.

§§ To whom correspondence should be addressed. Tel.: 33-2-40-08-47-23; Fax: 33-2-40-35-66-97; E-mail: yjacques@nantes.inserm.fr.

[1] The abbreviations used are: IL, interleukin; rIL, recombinant IL; IL-15Rα, IL-15 receptor α chain; NK, natural killer; GM-CSF, granulocyte macrophage-colony-stimulating factor; mAb, monoclonal antibody; ELISA, enzyme-linked immunosorbent assay; RIA, radioimmunoassay; DHFR, dihydrofolate reductase; PPL, preprolactin; WT, wild type.

This is an Open Access article under the CC BY license.

some of them respond to IL-15 (17, 18), suggesting the existence of new functional IL-15 receptor complexes not involving IL-2Rβ and/or IL-2Rγ. Distinct roles for IL-2 and IL-15 are also suggested from experiments in knock-out mice. Whereas IL-2−/− and IL-2Rα−/− mice develop exacerbated T and B cell expansion associated with autoimmune manifestations, IL-15−/− and IL-15Rα−/− mice on the contrary have normal T and B cell populations and display a profound defect in NK cells, NK-T cells, intraepithelial lymphocytes, and CD8+ memory T cells (19, 20). A recent study suggests that, contrary to the results obtained *in vitro*, the major role of IL-2 *in vivo* is to limit continuous expansion of activated T cells, whereas IL-15 is critical for initiating T cell division (21).

A number of studies have contributed to the identification of human disorders in which targeting the IL-15 system is of clinical relevance and potential benefit. Among them are autoimmune and inflammatory diseases, infectious diseases, transplant rejection, cancer, and immunodeficiencies (22, 23). In this context, the rational design of agonists or antagonists of the IL-15/receptor system is a major concern and requires precise knowledge of the structure of the high affinity IL-15 receptor complex.

A number of mutagenesis studies of human and murine IL-2 have led to the identification of several residues implicated in the binding to the IL-2Rα, -β, and -γ chains. From these studies, residues Lys-35, Arg-38, Phe-42, and Lys-43, all located in the A-B loop of human IL-2, are involved in its binding to the IL-2Rα chain, whereas residues Asp-20 on helix A and Asn-88 on helix C are involved in the binding to the IL-2Rβ chain, and Gln-126 on helix D is crucial for binding to the IL-2Rγ chain (24–26). Similar regions were identified on mouse IL-2 (27). On the contrary, very little data are available concerning the residues on IL-15 involved in the binding to the different IL-15 receptors. Some mutations in human IL-15 (Asp-8 and Gln-108), which are analogous to the ones described for human IL-2, suggested that the corresponding regions in IL-15 are involved in the binding to the IL-2Rβ and γ subunits, respectively (28).

In this study, we have used different complementary approaches, including ligand receptor interaction analysis, induction of biological activity, antibody mapping, peptide scanning, site-directed mutagenesis, and molecular modeling, to define the epitope of IL-15 responsible for high affinity binding to the IL-15Rα chain.

EXPERIMENTAL PROCEDURES

Cytokines and Antibodies—Recombinant murine IL-3 and human GM-CSF were purchased from R & D Systems (Abington, UK); recombinant human IL-15 (rIL-15) was purchased from PeproTech Inc (Rocky Hill, NJ), and recombinant human IL-2 (rIL-2) was purchased from Chiron (Emeryville, CA). Polyclonal goat anti-human IL-2 AF-202-NA was purchased from R & D Systems, and the mouse anti-human IL-2 mAb IL2.66 was from Immunotech (Marseille, France). Monoclonal mouse anti-human IL-15 MAB247 was obtained from R & D Systems, and mouse anti-human IL-15 mAb M111 was from Genzyme (Cambridge, MA). Monoclonal mouse anti-human IL-15Rα M161 was kindly provided by GenMab A/S (Copenhagen, Denmark), and mouse anti-FLAG mAb M2 conjugated to peroxidase was purchased from Sigma.

Cell Culture—All cells were grown in 5% CO_2 at 37 °C in a water-saturated atmosphere. The non-adherent TF-1 human cell line, TF-1β human cells (29) (kindly provided by Dr. Bruno Azzarone, IGR, Villejuif, France), and the adherent Chinese hamster ovary DUCKX cell line were cultured in a RPMI 1640 medium containing 10% heat-inactivated fetal calf serum, 2 mM glutamine, and specific reactants as follow: 1 ng/ml of GM-CSF (TF1); 1 ng/ml GM-CSF and 250 μg/ml geneticin (TF-1β); and 10 μg/ml adenosine, deoxyadenosine, and thymidine (DHFR−/− Chinese hamster ovary DUCKX). The non-adherent CTLL-2 murine cell line was cultured in an RPMI 1640 medium containing 8% fetal calf serum, 2 mM glutamine, 15 ng/ml rIL-2, and 50 μM 2-mercaptoethanol. Adherent 293-EBNA human cells (Invitrogen) were cultured in a Dulbecco's modified Eagle's medium containing 10% fetal calf serum, 2 mM glutamine, 1 mg/ml glucose, and 250 μg/ml geneticin.

Production of Anti-IL-15 Monoclonal Antibodies and Fab Fragments—The anti-IL-15 mAbs were produced following the immunization of BALB/c mice with recombinant human IL-15 (Diaclone, Besançon, France). Spleen cells were fused to the X6.3/AG.8653 myeloma according to conventional protocols. Hybridoma cloning was performed by limiting dilution, and the IgG-secreting clones were screened by ELISA on recombinant IL-15-coated wells for specific production of anti-IL-15 antibodies. Among the anti-IL-15 mAbs obtained, five were selected (B-T15, B-S19, B-P21, B-N22, and B-E29) that were all of the IgG1 isotype. They were produced in ascitic fluid and purified by ion exchange chromatography.

Fab fragments of anti-IL-15 B-E29 mAb were obtained by digestion with papain. B-E29 mAb was incubated for 2 h at 37 °C in phosphate-buffered saline with 20 mM cysteine, 20 mM EDTA, and 10 μg of papain/mg mAb. Iodoacetamide (75 mM final concentration) was added, and the reaction mixture was incubated at room temperature for 30 min. The Fab fragments were purified by size exclusion chromatography (Sephadex G-75 column).

Preparation of Soluble IL-15Rα-IL-2 Fusion Protein—To generate the chimeric soluble IL-15Rα-IL-2 construct, the signal peptide and the extracellular domain of IL-15Rα (nucleotides 1–697) were PCR-amplified from pNo15R (30), using the sense primer 5′-GGGAAGCTTAGTCCAGCGGTGTCCTGT-3′ (primer 1, nested HindIII restriction site underlined) and the antisense primer 5′-AACTGCAGAGTGGTGTCGCTGTGGCC-3′ (primer 2, PstI underlined). The amplified coding sequence was then cloned into a pBluescript plasmid coding for human IL-2 (31). In the final hybrid gene, the PstI site (coding for the dipeptide Leu-Gln) behaved as a linker between the IL-15Rα (5′ end) and IL-2 (3′ end) sequences. The sequence was controlled, and the chimeric construct was digested from the pBluescript plasmid between the HindIII/NotI sites and subcloned into the mammalian expression vector pKCR6 (32) at the EcoRI site. DHFR−/− Chinese hamster ovary cells were transfected with pKCR6-sIL-15Rα-IL-2 using SuperFect Reagent (Qiagen, Courtaboeuf, France). Clones producing the fusion protein were detected using an ELISA for detection of human IL-2 (BioSource, Nivelles, Belgium). Three rounds of cloning were performed using increasing concentrations of methotrexate (Sigma). One clone selected at 5 μM methotrexate produced about 4.3 mg/liter sIL-15Rα-IL-2. The supernatants were concentrated by precipitation with ammonium sulfate at 60% saturation and loaded onto an IL-2 immunoaffinity column (mAb IL2.66), and the IL-2 fusion protein was purified as described (31). Its concentration was determined by ELISA for human IL-2. Its purity was at least 80% with a molecular mass of 60 kDa, as assessed by SDS-PAGE after iodination with a chloramine-T method as described previously (12). Full functionality of the IL-2 portion of the fusion protein was demonstrated in a CTLL-2 proliferation assay (cell proliferation kit II, Roche Diagnostics), using rIL-2 as standard. High affinity IL-15 binding of the IL-15Rα portion was demonstrated by using the surface plasmon resonance technology (Biacore AB, Uppsala, Sweden).[2]

Production of IL-15 Mutants—The pEF-*neo* PPL signal peptide-IL-15 (human) expression construct was kindly provided by Dr. Yutaka Tagaya (33). The FLAG tag (DYKDDDDK) was introduced at the MluI site between the PPL signal peptide and the mature IL-15 protein coding sequence as a double-stranded oligonucleotide (5′-CGCGAGACTACAAGGATGACGATGACAAGT-3′ and 5′-CGCGACTTGTCATCGTCATCCTTGTAGTCT-3′). A pBluescript plasmid containing the PPL-FLAG-IL-15 sequence was generated by subcloning the ClaI/BamHI fragment. Amino acid switching was performed using the QuikChange Site-directed Mutagenesis Kit (Stratagene, La Jolla, CA) with the pBluescript construct. Sequences were confirmed over the PPL-FLAG-IL-15 hybrid cDNA, and the mutated ClaI/BamHI fragment was cloned back into pEF-*neo*. For the production of a FLAG-IL-15 mutant, 3.2×10^6 adherent 293-EBNA cells were transfected with 16 μg of the mutated IL-15 expression construct in a 60-mm plate following a standard calcium phosphate protocol. After 6 h, the medium was replaced with fresh complete Dulbecco's modified Eagle's medium (Invitrogen), and supernatants were harvested 48 h after transfection. The concentration of wild-type FLAG-IL-15 was determined in an RIA with the anti-IL-15 MAB247 as the coating antibody and iodinated anti-IL-15 mAb B-E29 as the revealing antibody, using commercial rIL-15 as standard. B-E29 mAb was radiolabeled with [^{125}I]iodine and IODO-GEN (Pierce) as catalyst (34), at a specific radioactivity of around 2000 cpm/fmol. The concentrations of FLAG-IL-15 mutants were then determined in an

[2] J. Bernard, unpublished results.

ELISA with MAB247 as the coating antibody and peroxidase-conjugated anti-FLAG M2 mAb as the revealing antibody, using wild-type FLAG-IL-15 as standard. The mutants were also tested in the RIA.

Pepscan Analysis—The overlapping synthetic peptides were synthesized and screened using credit card format mini-PEPSCAN cards (455 peptide format/card) as described previously (35). The binding of antibodies to each peptide was tested in a PEPSCAN-based ELISA. The 455-well credit card format polyethylene cards, containing the covalently linked peptides, were incubated at 4 °C overnight with the samples (mouse monoclonal anti-IL-15 antibody or soluble IL-15Rα-IL-2 fusion protein) diluted in blocking solution containing 5% horse serum (v/v) and 5% ovalbumin (w/v). After washing, the cards were incubated (1 h, 25 °C) with peroxidase-coupled rabbit anti-mouse IgGs at 1.3 μg/ml (P 0260, Dako Cytomation, Glostrup, Denmark) for anti-IL-15 antibody detection. For sIL-15Rα-IL-2 or rIL-2 detection, the cards were incubated with the anti-human IL-2 antibody AF-202-NA (1 μg/ml), washed, and further incubated with peroxidase-coupled rabbit anti-goat IgGs at 1.3 μg/ml (P 0160, Dako Cytomation). After washing, the peroxidase substrate 2,2′-azino-di-3-ethylbenzthiazoline sulfonate plus 2 μl/ml of 3% H_2O_2 were added, and the color development was quantified at 1 h, using a CCD camera and an image processing system. The set up consists of a CCD camera and a 55-mm lens (Sony CCD Video Camara XC-77RR, Nikon micro-nikkor 55-mm f/2.8 lens), a camera adaptor (Sony Camara adaptor DC-77RR), and the Image Processing software package Optimas, version 6.5 (Media Cybernetics, Silver Spring, MD), run on a Pentium II computer system. The CCD camera is equipped with an orange filter that translates the green color of the 2,2′-azino-di-3-ethylbenzthiazoline sulfonate substrate into gray values (arbitrary scale).

IL-15 Binding Assays—Human rIL-15 was radiolabeled with [^{125}I]iodine (specific radioactivity of around 2000 cpm/fmol) using a chloramine-T method (36), and binding experiments were performed as described previously (12). Nonspecific binding was determined in the presence of 100-fold excess of unlabeled cytokine. For the IL-15 binding experiments, TF-1 cells were incubated with increasing concentrations of labeled rIL-15. Regression analysis of the binding data was accomplished using a one-site equilibrium binding equation (Grafit, Erithacus Software, Staines, UK), and data were plotted in the Scatchard coordinate system. For inhibition of IL-15 binding experiments, TF-1 cells were incubated with a fixed concentration of iodinated rIL-15 and increasing concentrations of FLAG-IL-15 or mutants or mAbs. Regression analysis of data was accomplished using a 4-parameter logistic equation (Grafit, Erithacus Software).

Proliferation Assays—The proliferative inducing activity of FLAG-IL-15 and mutants and the inhibitory activity of mAbs were assessed by [^{3}H]thymidine incorporation on TF-1β cells. Cells were maintained in the culture medium for 3 days, washed twice, and starved for 2 h in the same medium without cytokine. They were plated at 10^4 cells in 100 μl and cultured for 48 h in the medium supplemented with increasing concentrations of rIL-15, FLAG-IL-15, or mutant or in the medium supplemented with a fixed concentration of rIL-15 and increasing concentration of mAbs. Cells were pulsed for 16 h with 0.5 μCi/well of [^{3}H]thymidine and harvested onto glass fiber filters, and cell-associated radioactivity was measured.

Sequence Alignment and Molecular Modeling—Sequences were obtained from the Swiss-Prot data base. Secondary structure prediction of human IL-15 was performed with PHD server (cubic.bioc.columbia.edu/predictprotein/submit_def.html). Sequence alignment with human IL-2 was generated automatically with the ClustalW program (37) and optimized manually under Seaview (38) according to conserved amino acids and predicted α-helical structure.

Homology modeling was performed with the Modeler module of InsightII (39) using the x-ray crystallographic structure of human IL-2 (Protein Data Bank code 1M47) as a template and the selected sequence alignment. Evaluation of the generated models was done by the Profiles_3D module of InsightII (40), Prosa II program (41), and PROCHECK program (42). The protein molecular surface of the selected model was defined using a solvent probe radius of 1.4 Å. The Engelman-Steitz scale was used to display the protein surface hydrophobicity (43).

RESULTS

Functional Properties of Anti-IL-15 mAbs—Seven anti-IL-15 mAbs were tested for interference with iodinated rIL-15 binding to IL-15Rα. The TF-1 cell line was chosen because it expresses cell-surface IL-15Rα and IL-2Rγ but not IL-2Rβ and, contrary to TF-1 cells transfected with IL-2Rβ (TF-1β), does not proliferate in response to IL-15. This cell line is therefore likely to express isolated membrane-associated IL-15Rα in the absence of IL-2Rβ/γ recruitment. TF-1 cells bound IL-15 with high affinity (K_d = 79 pM) (Fig. 1*B*), and the binding was completely abrogated by the anti-IL-15Rα mAb M161 (IC_{50} = 100 pM) (Fig. 1*A*), indicating that the binding indeed reflected the formation of an IL-15·IL-15Rα complex. Cross-linking studies have also shown the association of IL-15 with a single band corresponding to IL-15Rα.[3]

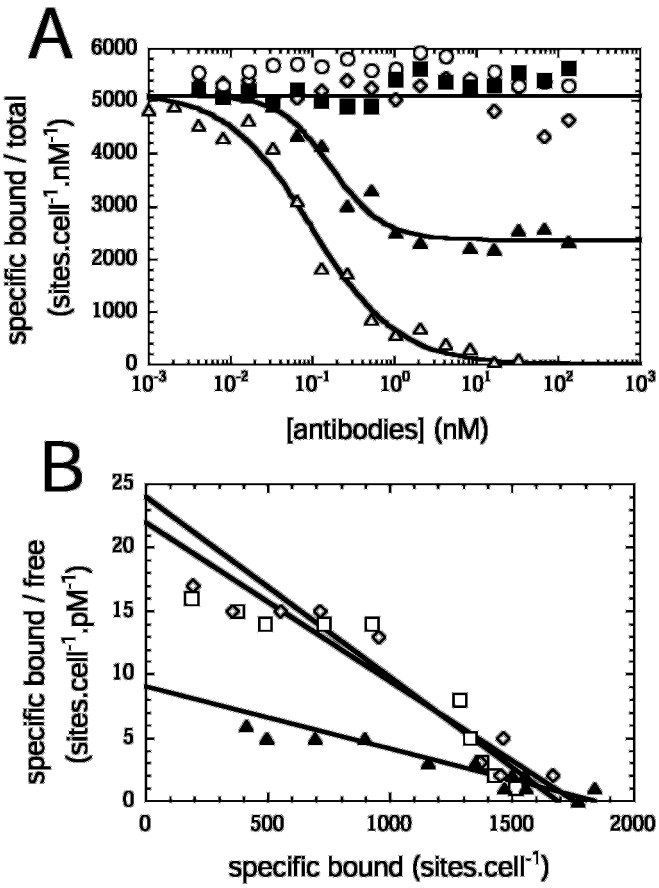

FIG. 1. **Effects of anti-IL-15 and anti-IL-15Rα mAbs on IL-15 binding to TF-1 cells.** *A*, TF-1 cells were equilibrated with a fixed concentration of radioiodinated rIL-15 (80 pM) and increasing concentrations (as indicated on the *abscissa*) of the following mAbs: anti-IL-15Rα mAb M161 (△), anti-IL-15 mAbs B-T15 (◇), B-E29 (▲), MAB247 (○), or M111 (■). The nonspecific cell binding component was determined in the presence of radioiodinated rIL-15 (80 pM) and a 100-fold excess (8 nM) of unlabeled rIL-15. Cell-bound and unbound (free) fractions were measured, and the specific bound fraction was calculated by subtracting the nonspecific binding from the cell-bound fraction. On the *ordinate* is plotted the ratio of the specific bound fraction (expressed in *sites·cell*$^{-1}$) over the total concentration (bound plus free) of radioiodinated rIL-15 (expressed in nM). *B*, TF-1 cells were equilibrated with increasing amounts of ^{125}I-labeled rIL-15 in the absence (□) or presence of 40 nM of B-T15 (◇) or B-E29 (▲) mAbs. The specific bound and unbound (free) fractions were determined as above.

Among the seven anti-IL-15 antibodies tested, only B-E29 inhibited IL-15 binding to this cell line. When tested on a fixed concentration of iodinated rIL-15 (Fig. 1*A*), the effect of B-E29 was dose-dependent, with an IC_{50} of 172 pM, and partial, with about 50% of IL-15 binding being resistant to the inhibitory effect of the antibody. In contrast, mAbs B-T15, MAB247, and M111 (shown in Fig. 1*A*), as well as mAbs B-S19, B-P21, and B-N22 (not shown), were without effect.

The partial inhibitory effect of B-E29 could reflect heterogeneity in IL-15Rα expressed by TF-1 cells, in that a fraction of receptors would bind IL-15 in a way sensitive to the inhibitory

[3] E. Mortier, unpublished results.

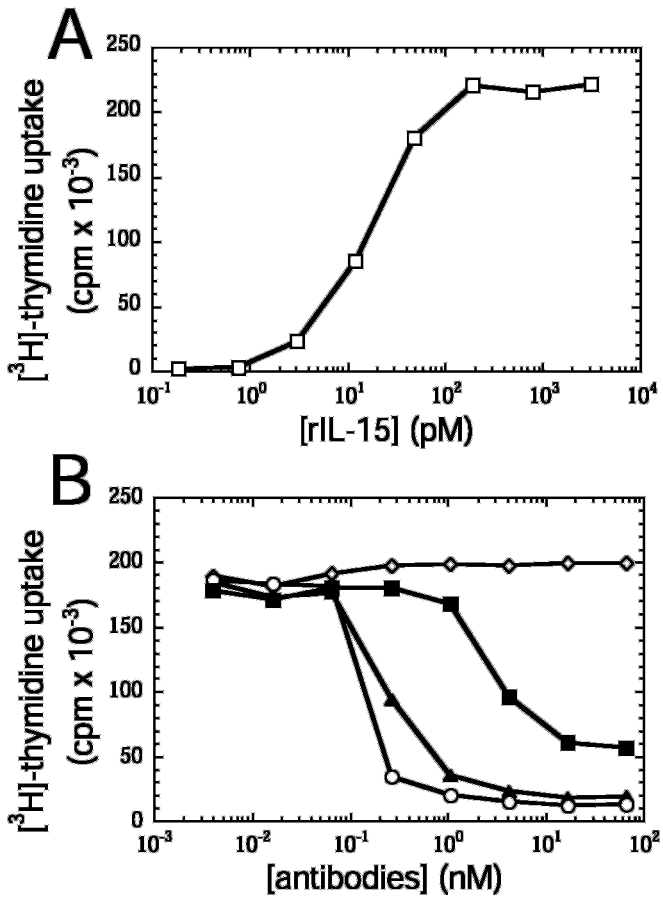

FIG. 2. **Effect of anti-IL-15 mAbs on IL-15-induced proliferation of TF-1β cells.** Cell proliferation was evaluated by measuring the incorporation of [^{3}H]thymidine. *A*, cells were cultured with increasing concentrations (as indicated on the *abscissa*) of rIL-15. *B*, cells were cultured with a fixed concentration of rIL-15 (200 pM) and increasing concentrations (as indicated on the *abscissa*) of anti-IL-15 mAbs: B-T15 (◇), B-E29 (▲), MAB247 (○), or M111 (■).

effect of the antibody, whereas the other fraction would not. Another possibility would be that B-E29 reduces the binding affinity of IL-15. To decide between these alternatives, B-E29 was tested at a saturating concentration (40 nM) on the IL-15 binding curve (Fig. 1*B*). Scatchard analysis of the binding curves showed that B-E29, contrary to B-T15, induced a homogeneous reduction of the affinity of IL-15 (K_d = 209 pM *versus* 79 pM in the absence of antibody). Similar results were obtained with Fab fragments of B-E29 (data not shown), suggesting that the effect of B-E29 did not involve cross-linking events.

The anti-IL-15 mAbs were next analyzed for their capacities to interfere with IL-15 induction of proliferation of the IL-15 dependent human TF-1β that expresses endogenous human IL-15Rα and IL-2Rγ together with transfected human IL-2Rβ (Fig. 2). As shown in Fig. 2*A*, this cell line dose-dependently responded to picomolar concentrations of IL-15, with an EC_{50} of 20 pM, reflecting the activation of high affinity IL-15Rα/IL-2Rβ/γ receptors. Among the series of seven anti-IL-15 antibodies tested, only B-E29, MAB247, and M111 were found to neutralize the effects of IL-15 on this cell line (Fig. 2*B*). The three mAbs induced dose-dependent inhibitory effects with IC_{50} values of 0.3, 0.13, and 4 nM, respectively, and the inhibitory effects of B-E29 and MAB247 were almost complete. The IC_{50} of B-E29 (0.3 nM) was in agreement with its inhibitory effect on IL-15 binding to TF-1 cells (IC_{50} = 0.172 nM).

Epitope Mapping of the Anti-IL-15 mAbs Using a Pepscan Technology—In a first attempt to identify the epitopes recognized by the anti-IL-15 mAbs, they were tested for their reactivity with IL-15 peptides using a peptide scanning technology. A series of 12-mer overlapping peptides shifted from one to the next by one amino acid and covering the entire sequence of human IL-15 (shown in Fig. 3*B*) were synthesized on a solid phase and assayed for anti-IL-15 mAb binding by using a two-step ELISA as described under "Experimental Procedures." With the inhibitory B-E29 antibody, a clear peak of reactivity was observed (Fig. 3*A*) that corresponded to the recognition of the peptide sequence ^{61}DTVENLIILANN^{72}, a peptide belonging to the predicted C-helix of IL-15 (Fig. 3*B*). A control experiment using the secondary anti-mouse antibody in the absence of B-E29 gave background reactivity (not shown). Given the inhibitory effects of B-E29, this peptidic sequence is therefore very likely to be involved in the binding of IL-15 to the IL-15Rα chain.

The reactivity of MAB247 was also analyzed by pepscan. Although a higher background was noted, a major peak of reactivity was found with IL-15 peptides covering the C-terminal part (^{102}SFVHIVQMFIN^{112}) and corresponding to the end of the D-helix (Fig. 3*B*). Insofar as MAB247 did not inhibit IL-15 binding to the IL-15Rα chain, the C-terminal part of IL-15 is therefore not implicated in this binding event. However, given the properties of MAB247 (inhibition of IL-15 induced proliferation without effect on IL-15 binding to IL-15Rα), this C-terminal helix is likely to participate in the recruitment of the transducing IL-2Rβ/γ complex. The M111 mAb that displayed similar functional features as MAB247 (no inhibition of IL-15 binding and inhibition of proliferation) was also found to cross-compete with MAB247 for binding to IL-15 (not shown), suggesting that these two antibodies recognize a common epitope. However, M111 did not show any reactivity in the pepscan studies, a result that could be due to the fact that M111 has a 5-fold lower affinity for IL-15 than MAB247 (not shown).

The anti-IL-15 mAbs B-T15 and B-P21 (Fig. 3*A*) gave strong peaks of reactivity located in the same region of IL-15. The anti-IL-15 mAb B-N22 gave a pattern very similar to that of B-T15 (not shown), and mAb B-S19 gave a pattern very similar to that of B-P21 (not shown). These four non-neutralizing antibodies therefore reacted with a region of IL-15 different from that recognized by B-E29 or MAB247. This region corresponded to the peptide sequence ^{85}CKECEELEEKN^{95} that is located in the loop between the predicted C and D helices (Fig. 3*B*). Therefore, this C-D loop is not likely to be involved in the binding and recruitment by IL-15 of IL-15 receptor components.

Analysis of IL-15Rα Binding to IL-15 by a Pepscan Approach—The pepscan approach was further used in an attempt to identify IL-15 regions directly involved in IL-15Rα binding. For that purpose, a soluble fusion protein (sIL-15Rα-IL-2) consisting of the extracellular domain of human IL-15Rα fused to human IL-2 was assayed for binding to the 12-mer IL-15 peptides, using a polyclonal anti-human IL-2 antibody (AF-202-NA) as the revealing antibody (Fig. 3*A*). Two main peaks of reactivity were observed that corresponded to the binding of sIL-15Rα-IL-2 with two different regions of the IL-15 sequence. Control experiments with a similar concentration (330 nM) of rIL-2 gave background reactivity (Fig. 3*A*). Pepscan studies on 30-mer peptides of human IL-15 confirmed the reactivity of sIL-15Rα-IL-2 with these two IL-15 regions (data not shown). Analysis of the two sets of reactive peptides (12-mer and 30-mer) allowed to assign the following sequences as responsible for sIL-15Rα-IL-2 binding: ^{44}LLELQVISL^{52} (peptide 1) and ^{64}ENLII^{68} (peptide 2). The first sequence is located within helix B (Fig. 3*B*). The second sequence, located in helix C, is completely contained in the one recognized by the mAb B-E29, a

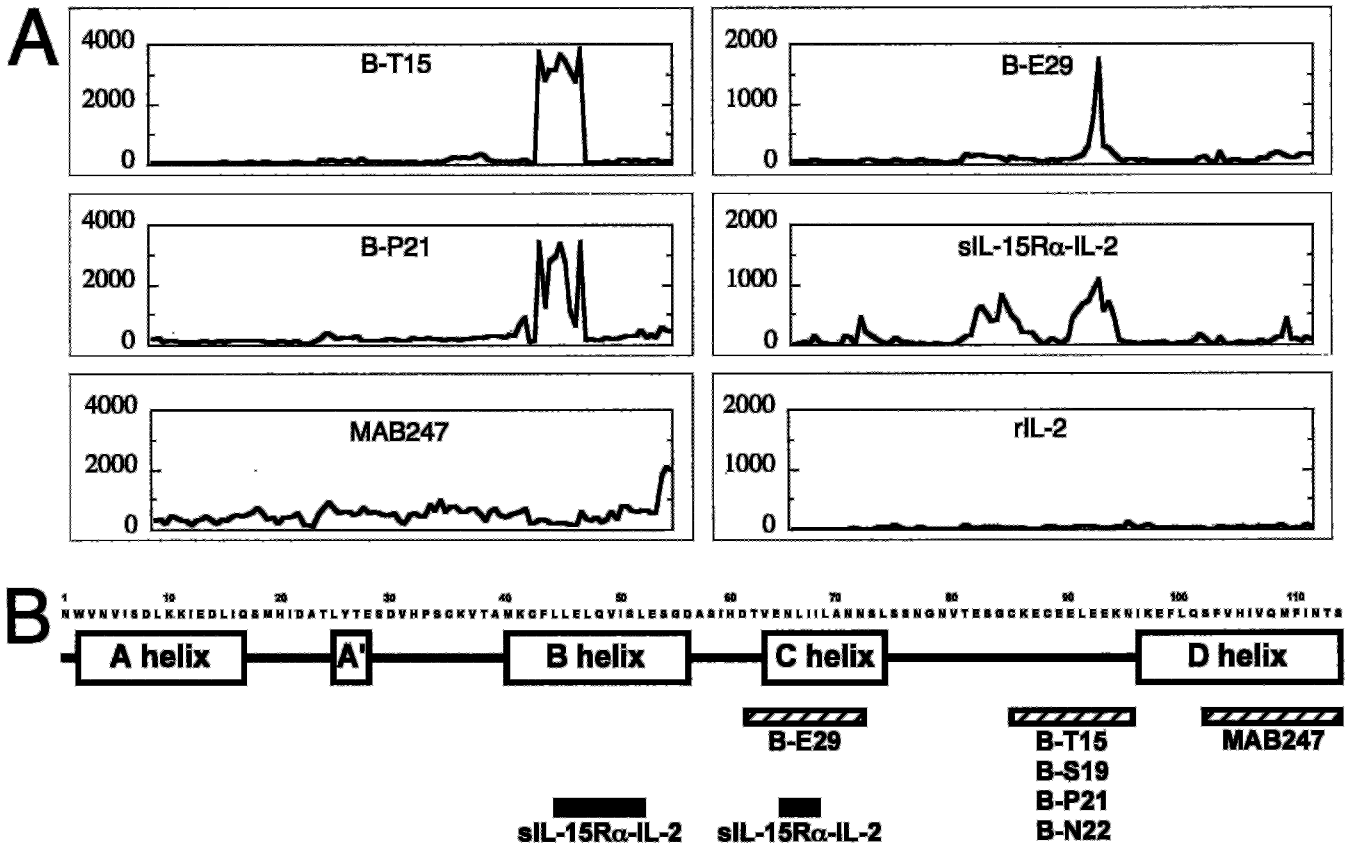

FIG. 3. **Analysis of the binding of anti-IL-15 mAbs and sIL-15Rα-IL-2 to IL-15 12-mer peptides.** *A*, 12-mer peptides spanning the entire amino acid sequence of human IL-15 were immobilized in multiwell plates and tested for their reactivity with the different molecules as indicated. The *left side* of each sub-panel corresponds to the N-terminal 12-mer peptide of IL-15. The anti-IL-15 mAbs were incubated at 10 μg/ml (B-P21 and B-E29; B-S19, B-N22, M111; not shown) or 1 μg/ml (MAB247 and B-T15), and their binding was revealed with peroxidase-coupled rabbit anti-mouse IgG. The sIL-15Rα-IL-2 fusion protein (20 μg/ml, *i.e.* 330 nM) or rIL-2 (5 μg/ml, *i.e.* 330 nM) was incubated, and their binding was revealed with the goat AF-202-NA anti-human IL-2 antibody plus a peroxidase-coupled rabbit anti-goat IgG. The reactivity of each well (*ordinates*, arbitrary scale) is measured as described under "Experimental Procedures." *B*, the peptide regions of human IL-15 recognized by the anti-IL-15 mAbs and sIL-15Rα-IL-2 are positioned on the primary structure of IL-15. The four α-helices predicted from our molecular model (see "Experimental Procedures" and Fig. 6*A*) are shown.

result that fits with and can explain the inhibitory potency of the antibody on IL-15 binding.

IL-15 Site-directed Mutagenesis—In order to confirm the involvement of the two peptidic regions identified by pepscan in the binding to the IL-15Rα chain, point mutations of IL-15 in these regions were carried out. In order to introduce a substantial disturbance in the presumed receptor-binding site, nonpolar hydrophobic side chains (Leu, Val, and Ile) and noncharged polar side chains (Ser, Gln, and Asn) were replaced by charged groups (Asp, Glu, or Lys), and charged polar side chains (Glu) were replaced by oppositely charged groups (Lys). Mutants were generated at positions 44–52 (peptide 1) and positions 64–68 (peptide 2). Wild-type human IL-15 and mutants were expressed as fusion proteins with an N-terminal FLAG peptide in the 293-EBNA cells. In order to determine their concentrations in 293-EBNA cell supernatants, specific assays were set up (see "Experimental Procedures" and below).

FLAG-IL-15 and mutants expressed in 293-EBNA cell supernatants were first assayed for their reactivities with anti-IL-15 mAbs (data not shown). Two assays were set up. The first one was a sandwich ELISA using MAB247 as capture antibody and peroxidase-labeled anti-FLAG (M2) mAb as sensor. The second was a sandwich RIA in which MAB247 was used as capture antibody and radioiodinated mAb B-E29 as sensor (see details under "Experimental Procedures"). FLAG-IL-15 and mutants were all recognized in the ELISA, in agreement with our finding under pepscan that MAB247 reacted with a region of IL-15 distinct from peptides 1 and 2. FLAG-IL-15 and most mutants in the peptide 1 region showed similar reactivities in the ELISA and RIA, indicating that they are similarly recognized by iodinated B-E29 mAb. By contrast, none of the FLAG-IL-15 analogs mutated in the peptide 2 region reacted in the RIA, a result that confirms the involvement of peptide 2 in the B-E29 binding epitope.

FLAG-IL-15 and mutants were then assayed for their ability to bind IL-15Rα expressed by TF-1 cells. For that purpose, a competition assay was used that allowed us to compare the efficiencies of the different mutants to inhibit the binding of a low, non-saturating concentration of radioiodinated rIL-15 to TF-1 cells. The competition curves are shown in Fig. 4, and the concentrations of mutants giving half-maximal inhibitory effects (IC_{50} values) are listed in Table I. FLAG-IL-15 inhibited labeled rIL-15 binding with an IC_{50} of 26 pM, a value in agreement with the equilibrium dissociation constant reflecting the binding of labeled rIL-15 to the same cells (K_d = 79 pM, Fig. 2*B*). This finding supports the validity of the competition assay to estimate the affinities of the different mutants. Mutations at three positions (Glu-46, Val-49, and Ile-50) within peptide 1 had profound effects on the affinity of IL-15, whereas mutation Q48K was without effect. Mutations at position Leu-45 (L45D and L45E), Ser-51, and Leu-52 reproducibly resulted in an increased (2–3-fold) affinity of IL-15 in this competition assay. The mutants L44D and L47D could not be evaluated in this assay because of production levels that were too low in 293-

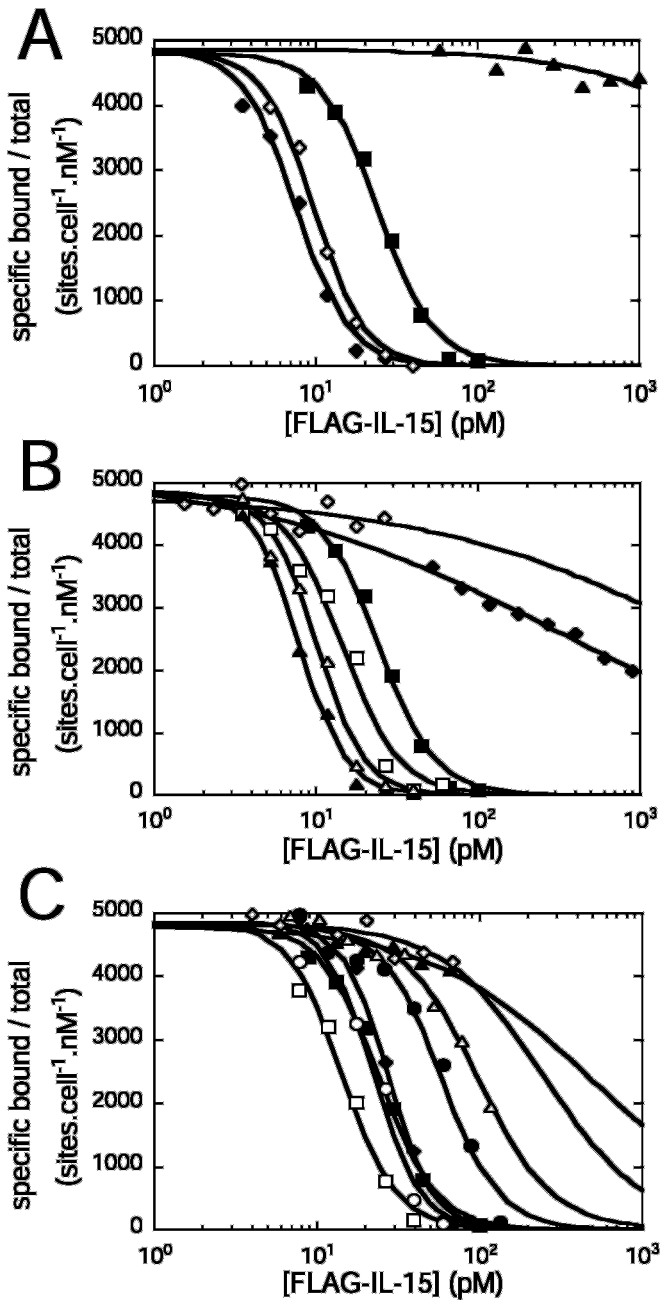

FIG. 4. **Determination of the affinities of FLAG-IL-15 and mutants for IL-15Rα by competition binding studies.** TF-1 cells were equilibrated with a fixed concentration (80 pM) of ^{125}I-rIL-15 and increasing concentrations (as indicated on the *abscissa*) of the FLAG-IL-15 wild type (WT) or mutants. *A*, WT (■), L45D (♦), L45E (◇), and E46K (▲). *B*, WT (■), Q48K (□), V49D (♦), I50D (◇), S51D (▲), and L52D (△). *C*, WT (■), E64K (□), N65K (♦), L66D (◇), L66E (▲), I67D (△), I67E (●), and I68D (○). Specific rIL-15 cell binding was calculated and plotted as described in the legend of Fig. 1*B*.

EBNA supernatants. Some mutations in the peptide 2 region (those directed to residues Leu-66 and Ile-67) also strongly reduced the affinity of IL-15, whereas mutations at positions Glu-64, Asn-65, and Ile-68 were without significant effects.

Wild-type FLAG-IL-15 and mutants were then tested for their growth-promoting effects on the IL-15-responsive TF-1β cells (Fig. 5 and Table II). The peptide 1 mutants displayed biological activities that correlated well with their IL-15Rα binding efficiencies measured on TF-1 cells; the L44D, E46K, L47D, and I50D mutations resulted in a strong reduction of the biological activity of IL-15, whereas mutation Q48K was without significant effect, and mutations at positions Leu-45, Ser-51, and Leu-52 induced a 2–4-fold increase in bio-activity. The only exception was mutant V49D which, despite a strongly reduced binding capacity, displayed nearly wild-type bio-activity.

TABLE I
Binding properties of the IL-15 mutants on the TF-1 cell line
Mean ± S.D. of the relative activities are from three independent experiments. ND, not determined; NA, not applicable.

FLAG-IL-15 proteins	IC_{50}	Relative activity
	pM	*% WT*
WT	26.1	100
L44D	ND	NA
L45D	10.1	258 ± 30
L45E	12.5	209 ± 10
E46K	13314.7	0.20 ± 0.01
L47D	ND	NA
Q48K	20.5	127 ± 27
V49D	347.7	8 ± 2
I50D	2949.8	0.88 ± 0.45
S51D	11.6	225 ± 36
L52D	10.9	239 ± 5
E64K	18.2	143 ± 43
N65K	26.6	98 ± 26
L66D	190.9	14 ± 8
L66E	407.1	6 ± 2
I67D	104.8	25 ± 6
I67E	63.7	41 ± 9
I68D	20.2	129 ± 28

In contrast, the correlation between biological activity on TF-1β cells and binding affinity on TF-1 cells was far weaker with mutants in the peptide 2 region. Mutant N65K, which displayed a nearly wild-type binding affinity on TF-1 cells, was inactive on TF-1β cells. Mutants E64K and I68D, which also displayed nearly wild-type binding affinities, behaved as partial agonists on TF-1β with maximal responses being about 20% that of wild-type IL-15. The only correlation was found for mutations at the Leu-66 and Ile-67 positions. The mutants L66D, L66E, I67D, and I67E displayed reduced bio-activity with a ranked order of potencies similar to that seen in the competition binding assay.

Molecular Modeling—The final alignment of IL-15 sequence to that of IL-2 is shown on Fig. 6*A*. Based on this alignment, the two cytokines share a 21.93% sequence identity. IL-15 sequence contains two disulfide bonds at positions Cys-42 to Cys-85 and Cys-35 to Cys-88, the former being homologous to the Cys–Cys within IL-2. The sequence alignment reveals conserved residues especially in helical structure supporting the structural homology of the two cytokines: DL*XXL*X*XX*I (*X* representing a non-conserved residue), C*XXX*EL, LI*XXX*N, and EFL*XXXXXXX*Q*XX*I in the A—D-helices, respectively. Two conserved residues (Asp-20 and Gln-126 of the IL-2 sequence) known to be involved in IL-2Rβ and IL-2Rγ binding, respectively, suggest similar interactions with those receptor subunits (44).

With this alignment, and based on the x-ray structure of human IL-2, three-dimensional models of human IL-15 were generated by Modeler program and tested for their accuracy using the three-dimensional-one-dimensional profile method (45), which calculates the local compatibility between a residue and its structural environment. The model given the best global score (S = 38.1) was retained. This score is close to that obtained for the template (S = 43.63) and is in agreement with a compilation of values obtained for correctly folded proteins of the same length (40). Two successive refinements were performed around two slim and weak mis-folded regions. The orientation of the side chains was then optimized with SCWRL3 program (46) using a backbone-dependent rotamer library. Energy minimization was then carried out with

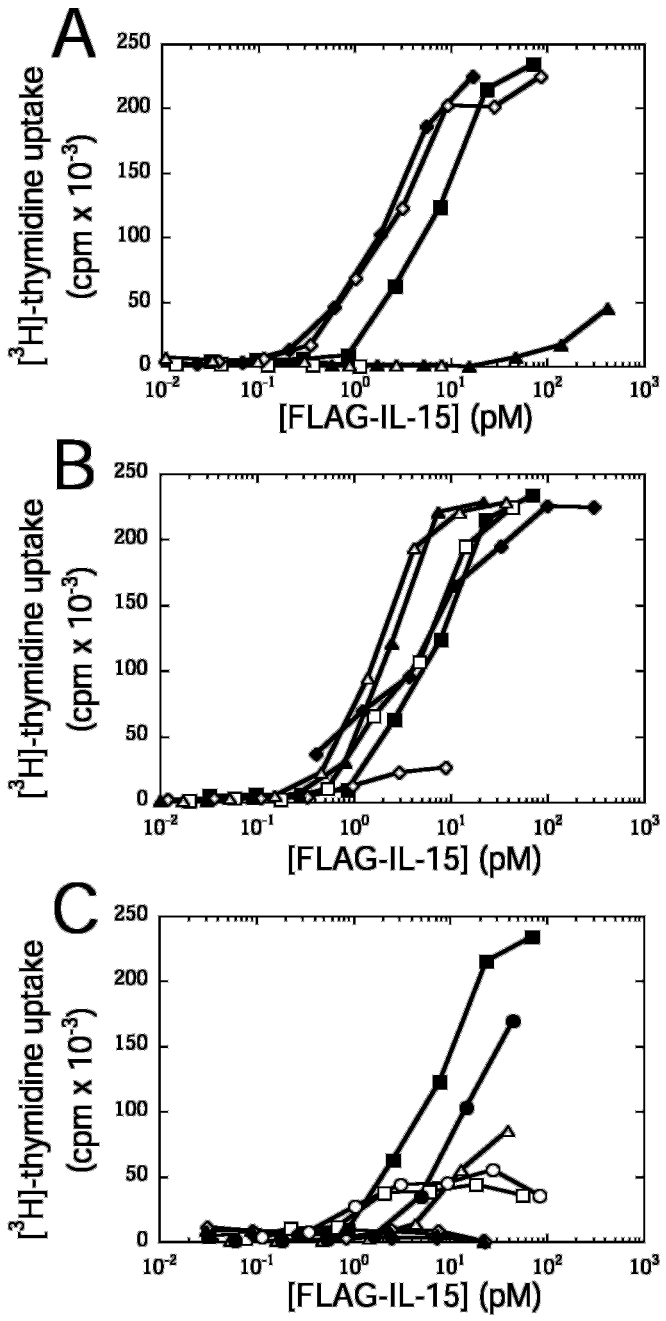

FIG. 5. **Proliferative activities of FLAG-IL-15 and mutants on TF-1β cells.** TF-1β cells were cultured in the presence of increasing concentrations (as indicated on the *abscissa*) of FLAG-IL-15 wild type (WT) or mutants. *A*, WT (■), L44D (□), L45D (♦), L45E (◇), E46K (▲), and L47D (△). *B*, WT (■) Q48K (□), V49D (♦), I50D (◇), S51D (▲), and L52D (△). *C*, WT (■), E64K (□), N65K (♦), L66D (◇), L66E (▲), I67D (△), I67E (●), and I68D (○). Cell proliferation was evaluated by measuring the incorporation of [^{3}H]thymidine.

CHARMm module (47) of Insight II and CFF force field (48), using Steepest Descents and adopted basis Newton-Raphson methods and a fixed backbone. A definitive evaluation of the optimized model was done using Profile three-dimensional ProsaII and PROCHECK. The three-dimensional profile plots were always larger than zero, indicating that most residues lie in a correct environment, and gave a global compatibility score of 40.2. The energy scores given by ProsaII were in accordance with those of the template. Furthermore, the stereochemical quality of the selected predicted model as evaluated by PROCHECK compares favorably with the template; the Ramachandran plot showed 89.8% residues in most favored regions, 7.4% in additional allowed regions, and 2.8% in generously allowed regions. A ribbon representation of the final model is shown in Fig. 6*B*, where peptide 1 and peptide 2 residue side chains are displayed. Because of the folding of the protein, helices B and C of IL-15 appear to be in close proximity. On Fig. 6*C* a Connolly surface representation is shown demonstrating that residues from peptides 1 and 2 are exposed to solvent (except Ile-50 which is buried in the core of the molecule) and form a continuous surface area. Hydrophobicity analysis (Fig. 6*D*) reveals that this area is composed of a large hydrophobic cluster containing four hydrophilic amino acids (Glu-46, Gln-48, Glu-64, and Asn-65).

TABLE II
Proliferative activities of the IL-15 mutants on TF-1β cells
Mean ± S.D. of the relative activities are from three independent experiments. NA, not applicable.

FLAG-IL-15 Proteins	Maximal induction	EC_{50}	Relative activity
	% WT	*pM*	*% WT*
WT	100	6.0	100
L44D	0	>20.0	<30
L45D	100	1.7	353 ± 73
L45E	100	2.4	250 ± 21
E46K	>20	>1300.0	<0.5
L47D	0	>60.0	<10
Q48K	100	4.8	125 ± 22
V49D	100	6.2	97 ± 55
I50D	>10	>60.0	<10
S51D	100	1.9	316 ± 26
L52D	100	1.7	353 ± 91
E64K	20	≈0.8	NA
N65K	0	>200.0	<0.4
L66D	0	>200.0	<0.4
L66E	0	>200.0	<0.4
I67D	>40	>30.0	<3
I67E	>75	>10.0	<8
I68D	20	≈0.8	NA

DISCUSSION

As opposed to the IL-2Rα chain that binds IL-2 with low affinity (49), the IL-15Rα chain has been shown *per se* to display high affinity binding for IL-15 (11). The interface between IL-15 and IL-15Rα therefore likely contributes to most of the free energy of binding of IL-15 to its functional high affinity (αβγ) receptor. To design proteins with agonist or antagonist properties of the IL-15 system, a good knowledge of the molecular features of the IL-15/IL-15Rα interface is therefore desirable. No data are available so far on that topic, and the main aim of this study was to contribute to the definition of the epitope in IL-15 responsible for the binding of IL-15Rα.

Two regions were first identified by pepscan that specifically bind a soluble form of IL-15Rα. They are positioned in Fig. 6 on a model of human IL-15 that was generated based on a sequence alignment with human IL-2. The first region (^{44}LLELQVISL^{52}, peptide 1) is located in the B-helix, and the second region (^{64}ENLII^{68}, peptide 2) belongs to the C-helix. The involvement of peptide 2 region in receptor binding was further supported by the fact that mAb B-E29, the only mAb among those tested that inhibits IL-15 binding to the IL-15Rα, reacts with a sequence (^{61}DTVENLIILANN^{72}) overlapping that of peptide 2. Two other epitopes could be defined; an antigenic region (^{85}CKECEELEEKN^{95}) located on the C-D loop was found to be shared by four non-inhibitory mAbs (B-T15, B-S19, B-P21, and B-N22) and is therefore not likely to be involved in receptor binding. MAB247 was found to inhibit IL-15-induced proliferation but not IL-15 binding to IL-15Rα, suggesting that it interfered with IL-2Rβ and/or IL-2Rγ recruitment. In pepscan experiments, MAB247 reacted with a sequence (^{102}SFVHIVQMFIN^{112}) located in helix D of IL-15. These find-

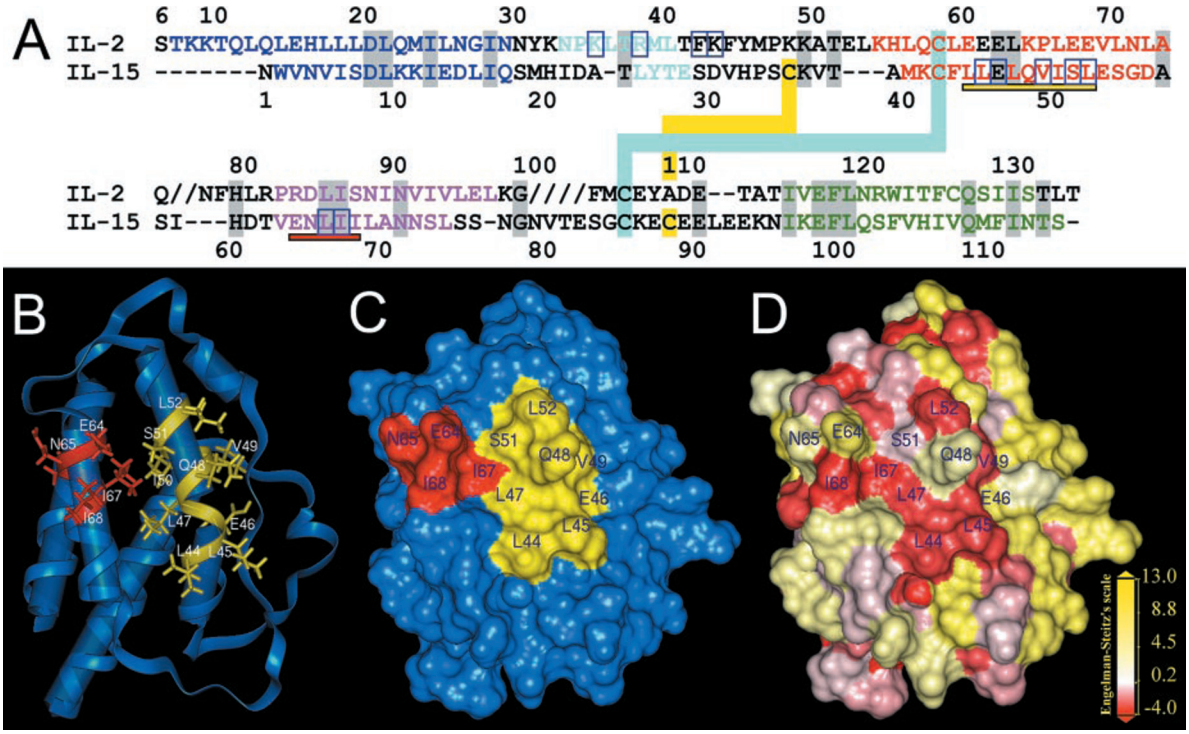

FIG. 6. **Sequence alignment for human IL-15 and IL-2 and molecular model of human IL-15.** *A*, α-helices are identified by *colored letters* (*helix A*, *dark blue*; *A′*, *light blue*; *B*, *red*; *C*, *pink*; *D*, *green*). The disulfide bridge common to IL-2 and IL-15 is shown in *blue*, and the proposed disulfide bridge specific to IL-15 is shown in *yellow*. Conserved amino acids between IL-2 and IL-15 are *shaded* in *gray*. On the IL-2 sequence, / indicates a missing residue in the 1M47 Protein Data Bank structure. On the IL-15 sequence, residues *underlined* in *yellow* or *red* correspond to amino acids in peptide 1 or 2, respectively. *Open blue boxes* indicate human IL-2 or IL-15 residues that have been shown to participate in IL-2Rα binding (25) or to be involved in the binding to IL-15Rα (this paper), respectively. *B*, the side chains of the ribbon drawing shown in *yellow* or *red* color correspond to the residues in peptide 1 or 2, respectively. *C*, the Connolly surfaces of modeled IL-15 colored in *yellow* or *red* correspond to amino acids in peptide 1 or 2, respectively. *D*, the Connolly surfaces of modeled IL-15 are colored according to the hydrophobicity index of the exposed residues (hydrophobic in *red*; hydrophilic in *yellow*).

ings agree well with the fact that this region, particularly residue Gln-108, has been suggested to be involved in the recruitment of the IL-2Rγ chain (28).

Mutagenesis studies confirmed the involvement of these two regions and enabled us to identify amino acids that participate in receptor binding and induction of bio-activity. Within the first region (peptide 1), and according to our structural model (Fig. 6*C*), Ile-50 is the only amino acid to be completely buried in the hydrophobic core of IL-15 and is therefore unlikely to be accessible for the receptor. Mutation at that position (I50D) strongly reduced the ability of IL-15 to bind to IL-15Rα as well as to induce cell proliferation, a result that might reflect a local conformational change that affects binding and signaling. However, this conformational change seems not to disturb the overall structure of the molecule, as far as the I50D mutant was found to be recognized by MAB247 in the ELISA. Among the solvent-exposed residues in peptide 1 (Fig. 6*C*), Glu-46, Val-49, Leu-45, Ser-51, and Leu-52 were found to be involved in IL-15Rα binding. Glu-46 was crucial, because replacement of its acidic side chain by a basic one (E46K) resulted in a complete loss of IL-15 binding to IL-15Rα and bio-activity. Replacement of the hydrophobic side chain of Val-49 by a negatively charged side chain (V49D) also resulted in a strong (13-fold) reduction of the affinity of IL-15 for IL-15Rα. Unexpectedly, the V49D mutant showed almost wild-type biological activity. A similar discrepancy between binding affinity and bio-activity has been reported for an IL-2 mutant (T51P) (50). This mutant was as active as wild-type IL-2, although it displayed a 10-fold lower receptor binding affinity. It has been shown that this mutant was deficient in inducing internalization of high affinity receptors, thus resulting in longer duration of receptor occupancy and induction of biological response. Whether the V49D IL-15 analog exhibits similar properties needs further investigation.

Mutations at positions Leu-45, Ser-51, and Leu-52 did not result in reduction but to an increase in binding and bio-activity, indicating that these residues are also involved in IL-15Rα binding. The mutants L44D and L47D showed impaired biological responses, although their binding affinity could not be evaluated. Unexpected, mutant Q48K showed almost wild-type properties, although Gln-48 is positioned in the center of an epitope formed by amino acids (Leu-45, Glu-46, Val-49, Ser-51, and Leu-52) which participate in receptor binding. Additional mutations of that residue might be required to reassess its potential involvement in receptor binding.

The results of mutagenesis in the peptide 2 region showed that among the five amino acids evaluated (Glu-64 to Ile-68), only Leu-66 and Ile-67, which are partially solvent-exposed (Fig. 6*C*), seem to be involved in receptor binding. The mutants (L66D, L66E, I67D, and I67E) displayed reduced binding affinities and corresponding reductions of their biological activities. Mutants E64K and I68D had affinities similar to that of wild-type IL-15, suggesting that Glu-64 and Ile-68 are not involved in IL-15Rα binding. However, the mutants behaved as partial agonists in the proliferation assay. Because partial agonism is indicative of defective activation of the receptor (51), Glu-64 and Ile-68 might be involved in the recruitment of the IL-2Rβ/γ transduction complex. This conclusion might hold for Asn-65 whose mutation (N65K) resulted in a loss of bio-activity without detectable alteration of the IL-15Rα binding affinity. Mutagenesis of mouse IL-2 and molecular modeling studies (27, 52) has indicated that, in addition to residue Asp-20 located on helix A (24), the C-helix of human IL-2 is also potentially involved in its interaction with IL-2Rβ, and recent work has

shown that a mutation in that helix (N88R) resulted in a drastic (1000-fold) loss of IL-2 binding to IL-2Rβ (26). Our results suggest that the corresponding regions in human IL-15, especially residues Glu-64, Asn-65, and Ile-68, participate also in the recruitment of the IL-2Rβ chain.

The IL-15 mutants E64K, N65K, and I68D display properties (low or no biological activity despite high affinity binding to IL-15Rα) that designate them as potential IL-15 antagonists. Preliminary experiments[2] indeed indicate that N65K can inhibit IL-15-induced cell proliferation.

The region of IL-15 that corresponds to peptide 2 seems to participate both in IL-15Rα and IL-2Rβ binding. The functional properties of the B-E29 mAb strengthen this notion. Pepscan studies showed that peptide 2 (^{64}ENLII^{68}) belongs to the epitopic region of B-E29, and mutagenesis revealed that all amino acids of peptide 2 (Glu-64 to Ile-68) are involved in this process. B-E29 inhibited both IL-15 binding to IL-15Rα and IL-15-induced proliferation through the IL-15Rα-IL-2Rβ/γ high affinity complex. However, although it only partially affected binding (about 3-fold reduction in the binding affinity of IL-15), it completely abrogated proliferation. A conclusion from these results is that B-E29, by blocking peptide 2 and especially amino acids Leu-66 and Ile-67, partially affects IL-15 binding to IL-15Rα, whereas by blocking amino acids Glu-64, Asn-65, and Ile-68, it completely blocks the recruitment of the IL-2Rβ chain.

The involvement of the epitope corresponding to peptide 2 in both IL-15Rα binding and IL-2Rβ recruitment might have implications on the dynamics of the receptor assembly. IL-15 would first bind with high affinity to IL-15Rα by engaging the peptide 1 and peptide 2 (or part) epitopes. Subsequent IL-2Rβ recruitment could then involve the engagement of another part of the peptide 2 epitope. Alternatively, a conformational change could occur in which IL-2Rβ would replace IL-15Rα in binding to the peptide 2 epitope.

In the case of mouse IL-2, a sequence of helix B analogous to the epitope in IL-15 corresponding to peptide 1 has been shown to interact with IL-2Rα (namely residues Glu-76, Pro-79, Val-83, and Leu-86) (27). In the case of human IL-2, no mutations in the B-helix that affect IL-2 binding to IL-2Rα have been described so far, although molecular modeling has predicted a contact between helix B of human IL-2 (namely residues Lys-64 and Glu-68 or Glu-61 and Glu-62) and IL-2Rα (52). In contrast, the region in IL-2 within helix C analogous to the epitope in IL-15 corresponding to peptide 2 does not appear to be involved in IL-2Rα binding (27). Our results therefore indicate that the mode of interaction of IL-15 with IL-15Rα is not completely homologous to the mode of interaction of IL-2 with IL-2Rα. This may reflect the fact that IL-15 displays an affinity for its α chain that is about 500-fold higher than the affinity of IL-2 for its α chain. In the case of human IL-2, the loop connecting helix A and helix B (namely residues Lys-35, Arg-38, Phe-42, and Lys-43) has been shown to participate in IL-2Rα binding (25). Although our pepscan studies did not show any significant binding of the soluble IL-15Rα to peptides that correspond to the A-B loop of IL-15, they remain to be validated by a mutational study.

In conclusion, we identified two regions in IL-15 that are involved in the binding to IL-15Rα, one of them being also used to recruit the IL-2Rβ transducing subunit. IL-15 muteins (L45D, L45E, S51D, and L52D), which display binding and biological properties higher than those of wild-type IL-15 and therefore behave as super-agonists, are valuable tools to expand lymphocyte subsets (*e.g.* NK cells, NK-T cells, and CD8+ memory T cells) and might be useful as therapeutic agents in patients with cancer or immunodeficiencies. Other muteins (E64K, N65K, and I68D) display properties that designate them as potential IL-15 antagonists and might be useful in inflammatory diseases like rheumatoid arthritis and generalized Shwartzman reaction where IL-15 is thought to play an important role (22).

REFERENCES

1. Grabstein, K. H., Eisenman, J., Shanebeck, K., Rauch, C., Srinivasan, S., Fung, V., Beers, C., Richardson, J., Schoenborn, M. A., Ahdieh, M., Johnson, L., Alderson, M. R., Watson, J. D., Anderson, D. M., and Giri, J. G. (1994) *Science* **264,** 965–968
2. Burton, J. D., Bamford, R. N., Peters, C., Grant, A. J., Kurys, G., Goldman, C. K., Brennan, J., Roessler, E., and Waldmann, T. A. (1994) *Proc. Natl. Acad. Sci. U. S. A.* **91,** 4935–4939
3. Sprang, S. R., and Bazan, J. F. (1993) *Curr. Opin. Struct. Biol.* **3,** 815–827
4. Carson, W. E., Giri, J. G., Lindeman, M. J., Linett, M. L., Ahdieh, M., Paxton, R., Anderson, D., Eisenmann, J., Grabstein, K., and Caligiuri, M. A. (1994) *J. Exp. Med.* **180,** 1395–1403
5. Armitage, R. J., Macduff, B. M., Eisenman, J., Paxton, R., and Grabstein, K. H. (1995) *J. Immunol.* **154,** 483–490
6. Wilkinson, P. C., and Liew, F. Y. (1995) *J. Exp. Med.* **181,** 1255–1259
7. Giri, J. G., Ahdieh, M., Eisenman, J., Shanebeck, K., Grabstein, K. H., Kumaki, A., Namen, A., Park, L. S., Cosman, D., and Anserson, D. M. (1994) *EMBO J.* **13,** 2822–2830
8. Anderson, D. M., Kumaki, S., Ahdieh, M., Bertles, J., Tometsko, M., Loomis, A., Giri, J., Copeland, N. G., Gilbert, D. J., Jenkins, N. A., Valentine, V., Shapiro, D. N., Morris, S. W., Park, L. S., and Cosman, D. (1995) *J. Biol. Chem.* **270,** 29862–29869
9. Norman, D. G., Barlow, P. N., Baron, M., Day, A. J., Sim, R. B., and Campbell, I. D. (1991) *J. Mol. Biol.* **219,** 717–725
10. Minami, Y., Kono, T., Miyasaki, T., and Taniguchi, T. (1993) *Annu. Rev. Immunol.* **11,** 245–267
11. Giri, J. G., Anderson, D. M., Kumaki, S., Park, L. S., Grabstein, K. H., and Cosman, D. (1995) *J. Leukocyte Biol.* **5745,** 763–766
12. Lehours, P., Raher, S., Dubois, S., Guo, J., Godard, A., and Jacques, Y. (2000) *Eur. Cytokine Netw.* **11,** 207–215
13. Johnston, J. A., Bacon, C. M., Finbloom, D. S., Rees, R. C., Kaplan, D., Shibuya, K., Ortaldo, J. R., Gupta, S., Chen, Y. Q., Giri, J. D., and O'Shea, J. J. (1995) *Proc. Natl. Acad. Sci. U. S. A.* **92,** 8705–8709
14. Miyasaki, T., Liu, Z.-J., Kawahara, A., Minami, Y., Yamada, K., Tsujimoto, Y., Barsoumian, E. L., Perlmutter, R. M., and Taniguchi, T. (1995) *Cell* **81,** 223–231
15. Bulanova, E., Budagian, V., Pohl, T., Krause, H., Durkop, H., Paus, R., and Bulfone-Paus, S. (2001) *J. Immunol.* **167,** 6292–6302
16. Pereno, R., Giron-Michel, J., Gaggero, A., Cazes, E., Meazza, R., Monetti, M., Monaco, E., Mishal, Z., Jasmin, C., Indiveri, F., Ferrini, S., and Azzarone, B. (2000) *Oncogene* **19,** 5153–5162
17. Bulfone-Paus, S. S., Bulanova, E., Pohl, T., Budagian, V., Durkop, H., Ruckert, R., Kunzendorf, U., Paus, R., and Krause, H. (1999) *FASEB J.* **13,** 1575–1585
18. Stevens, A. C., Matthews, J., Andres, P., Baffis, V., Zheng, X. X., Chae, D. W., Smith, J., Strom, T. B., and Maslinski, W. (1997) *Am. J. Physiol.* **272,** G1201–G1208
19. Kennedy, M. K., Glaccum, M., Brown, S. N., Butz, E. A., Viney, J. L., Embers, M., Matsuki, N., Charrier, K., Sedger, L., Willis, C. R., Brasel, K., Morrissey, P. J., Stocking, K., Schuh, J. C., Joyce, S., and Peschon, J. J. (2000) *J. Exp. Med.* **191,** 771–780
20. Lodolce, J. P., Burkett, P. R., Boone, D. L., Chien, M., and Ma, A. (2001) *J. Exp. Med.* **194,** 1187–1194
21. Li, X. C., Demirci, G., Ferrari-Lacraz, S., Groves, C., Coyle, A., Malek, T. R., and Strom, T. B. (2001) *Nat. Med.* **7,** 114–118
22. Fehniger, T. A., and Caligiuri, M. A. (2001) *Blood* **97,** 14–32
23. Fehniger, T. A., Cooper, M. A., and Caligiuri, M. A. (2002) *Cytokine Growth Factor Rev.* **13,** 169–183
24. Collins, L., Tsien, W. H., Seals, C., Hakimi, J., Weber, D., Bailon, P., Hoskings, J., Greene, W. C., Toome, V., and Ju, G. (1988) *Proc. Natl. Acad. Sci. U. S. A.* **85,** 7709–7713
25. Sauve, K., Nachman, M., Spence, C., Bailon, P., Campbell, E., Tsien, W. H., Kondas, J. A., Hakimi, J., and Ju, G. (1991) *Proc. Natl. Acad. Sci. U. S. A.* **88,** 4636–4640
26. Shanafelt, A. B., Lin, Y., Shanafelt, M. C., Forte, C. P., Dubois-Stringfellow, N., Carter, C., Gibbons, J. A., Cheng, S. L., Delaria, K. A., Fleischer, R., Greve, J. M., Gundel, R., Harris, K., Kelly, R., Koh, B., Li, Y., Lantz, L., Mak, P., Neyer, L., Plym, M. J., Roczniak, S., Serban, D., Thrift, J., Tsuchiyama, L., Wetzel, M., Wong, M., and Zolotorev, A. (2000) *Nat. Biotechnol.* **18,** 1197–1202
27. Zurawski, S. M., Vega, F. J., Doyle, E. L., Huyghe, B., Flaherty, K., McKay, D. B., and Zurawski, G. (1993) *EMBO J.* **12,** 5113–5119
28. Pettit, D. K., Bonnert, T. P., Eisenman, J., Srinivasan, S., Paxton, R., Beers, C., Lynch, D., Miller, B., Yost, J., Grabstein, K. H., and Gombotz, W. R. (1997) *J. Biol. Chem.* **272,** 2312–2318
29. Farner, N. L., Gan, J., de Jong, J. L., Leary, T. P., Fenske, T. S., Buckley, P., Dunlap, S., and Sondel, P. M. (1997) *Cytokine* **9,** 316–327
30. Dubois, S., Magrangeas, F., Lehours, P., Raher, S., Bernard, J., Boisteau, O., Leroy, S., Minvielle, S., Godard, A., and Jacques, Y. (1999) *J. Biol. Chem.* **274,** 26978–26984
31. Blanc, C., Vusio, P., Schleinkofer, K., Boisteau, O., Pflanz, S., Minvielle, S., Grotzinger, J., Muller-Newen, G., Heinrich, P. C., Jacques, Y., and Montero-Julian, F. A. (2000) *J. Immunol. Methods* **241,** 43–59
32. Matrisian, L. N., Bowden, G. T., Krieg, P., Fürstenberger, G., Briand, J. P., Leroy, P., and Breathnach, R. (1986) *Proc. Natl. Acad. Sci. U. S. A.* **83,**

9413–9417
33. Marks-Konczalik, J., Dubois, S., Losi, J. M., Sabzevari, H., Yamada, N., Feigenbaum, L., Waldmann, T. A., and Tagaya, Y. (2000) *Proc. Natl. Acad. Sci. U. S. A.* **97,** 11445–11450
34. Fraker, P. J., and Speck, J. C. (1978) *Biochem. Biophys. Res. Commun.* **80,** 849–857
35. Slootstra, J. W., Puijk, W. C., Ligtvoet, G. J., Langeveld, J. P., and Meloen, R. H. (1996) *Mol. Divers.* **1,** 87–96
36. Tejedor, F., and Ballesta, J. P. G. (1982) *Anal. Biochem.* **127,** 143–149
37. Thompson, J. D., Higgins, D. G., and Gibson, T. J. (1994) *Nucleic Acids Res.* **22,** 4673–4680
38. Galtier, N., Gouy, M., and Gautier, C. (1996) *Comput. Appl. Biosci.* **12,** 543–548
39. Sali, A., and Blundell, T. L. (1993) *J. Mol. Biol.* **234,** 779–815
40. Luthy, R., Bowie, J. U., and Eisenberg, D. (1992) *Nature* **356,** 83–85
41. Sippl, M. J. (1993) *Proteins* **17,** 355–362
42. Laskowski, R. A., Moss, D. S., and Thornton, J. M. (1993) *J. Mol. Biol.* **231,** 1049–1067
43. Engelman, D. M., and Steitz, T. A. (1981) *Cell* **23,** 411–422
44. Rozwarski, D. A., Gronenborn, A. M., Clore, G. M., Bazan, J. F., Bohm, A., Wlodawer, A., Hatada, M., and Karplus, P. A. (1994) *Structure* **2,** 159–173
45. Bowie, J. U., Luthy, R., and Eisenberg, D. (1991) *Science* **253,** 164–170
46. Canutescu, A. A., Shelenkov, A. A., and Dunbrack, R. L., Jr. (2003) *Protein Sci.* **12,** 2001–2014
47. Brooks, B. R., Bruccoleri, R. E., Olason, B. D., States, D. J., Swaminathan, S., and Karplus, M. (1983) *J. Comput. Chem.* **4,** 187–217
48. Maple, J. R., Hwang, M.-J., Jalkane, K. J., Stocktisch, T. P., and Hagler, A. T. (1998) *J. Comput. Chem.* **19,** 430–458
49. Greene, W. C., Robb, R. J., Svetlick, P. B., Rusk, C. M., Depper, J. M., and Leonard, W. J. (1985) *J. Exp. Med.* **162,** 363–368
50. Chang, D. Z., Wu, Z., and Ciardelli, T. L. (1996) *J. Biol. Chem.* **271,** 13349–13355
51. Black, J. (1989) *Science* **139,** 1550–1556
52. Bamborough, P., Hedgecock, C. J., and Richards, W. G. (1994) *Structure* **2,** 839–851